



Sirt1 protects against intervertebral disc degeneration induced by 1,25-dihydroxyvitamin D insufficiency in mice by inhibiting the NF- κ B inflammatory pathway



Peng Wang^{a,b,1}, Cuicui Yang^{b,1}, Jinhong Lu^b, Yongxin Ren^c, David Goltzman^d, Dengshun Miao^{b,*}

^a Department of Orthopaedics, Lianyungang Clinical College of Nanjing Medical University, The First People's Hospital of Lianyungang, Lianyungang, Jiangsu, China

^b The Research Center for Bone and Stem Cells, Department of Anatomy, Histology and Embryology, Nanjing Medical University, Nanjing, Jiangsu, China

^c Department of Orthopaedics, The First Affiliated Hospital of Nanjing Medical University, Nanjing, Jiangsu, China

^d Calcium Research Laboratory, McGill University Health Centre and Department of Medicine, McGill University, Montreal, Quebec, H4A 3J1, Canada

ARTICLE INFO

Keywords:

Vitamin D
Vitamin D receptor
Sirt1
Intervertebral disc degeneration
NF- κ B

ABSTRACT

Background: It has been demonstrated that vitamin D deficiency is associated with an increased risk of patients developing lumbar disc herniation. However, intervertebral disc degeneration caused by active vitamin D deficiency has not been reported. Thus, the purpose of this study was to investigate the role and mechanism of 1,25-dihydroxyvitamin D (1,25(OH)₂D) insufficiency in promoting intervertebral disc degeneration.

Methods: The phenotypes of intervertebral discs were compared in wild-type mice and mice with heterozygous deletion of 1 α -hydroxylase [1 α (OH)ase^{+/-}] at 8 months of age using iconography, histology and molecular biology. A mouse model that overexpressed Sirt1 in mesenchymal stem cells on a 1 α (OH)ase^{+/-} background (Sirt1^{Tg}/1 α (OH)ase^{+/-}) was generated by crossing Prx1-Sirt1 transgenic mice with 1 α (OH)ase^{+/-} mice and comparing their intervertebral disc phenotypes with those of Sirt1^{Tg}, 1 α (OH)ase^{+/-} and wild-type littermates at 8 months of age. A vitamin D receptor (VDR)-deficient cellular model was generated by knock-down of endogenous VDR using Ad-siVDR transfection into nucleus pulposus cells; VDR-deficient nucleus pulposus cells were then treated with or without resveratrol. The interactions between Sirt1 and acetylated p65, and p65 nuclear localization, were examined using co-immunoprecipitation, Western blots and immunofluorescence staining. VDR-deficient nucleus pulposus cells were also treated with 1,25(OH)₂D₃, or resveratrol or 1,25(OH)₂D₃ plus Ex527 (an inhibitor of Sirt1). Effects on Sirt1 expression, cell proliferation, cell senescence, extracellular matrix protein synthesis and degradation, nuclear factor- κ B (NF- κ B), and expression of inflammatory molecules, were examined, using immunofluorescence staining, Western blots and real-time RT-PCR.

Results: 1,25(OH)₂D insufficiency accelerated intervertebral disc degeneration by reducing extracellular matrix protein synthesis and enhancing extracellular matrix protein degradation with reduced Sirt1 expression in nucleus pulposus tissues. Overexpression of Sirt1 in MSCs protected against 1,25(OH)₂D deficiency-induced intervertebral disc degeneration by decreasing acetylation and phosphorylation of p65 and inhibiting the NF- κ B inflammatory pathway. VDR or resveratrol activated Sirt1 to deacetylate p65 and inhibit its nuclear translocation into nucleus pulposus cells. Knockdown of VDR decreased VDR expression and significantly reduced the proliferation and extracellular matrix protein synthesis of nucleus pulposus cells, significantly increased the senescence of nucleus pulposus cells and significantly downregulated Sirt1 expression, and upregulated matrix metalloproteinase 13 (MMP13), tumor necrosis factor- α (TNF- α) and interleukin 1 β (IL-1 β) expression; the ratios of acetylated and phosphorylated p65/p65 in nucleus pulposus cells were also increased. Treatment of nucleus pulposus cells with VDR reduction using 1,25(OH)₂D₃ or resveratrol partially rescued the degeneration phenotypes, by up-regulating Sirt1 expression and inhibiting NF- κ B inflammatory pathway; these effects in nucleus pulposus cells were blocked by inhibition of Sirt1.

Conclusion: Results from this study indicate that the 1,25(OH)₂D/VDR pathway can prevent the degeneration of nucleus pulposus cells by inhibiting the NF- κ B inflammatory pathway mediated by Sirt1.

* Corresponding author.

E-mail address: dsmiao@njmu.edu.cn (D. Miao).

¹ Equal contribution: These authors contributed equally to this work

<https://doi.org/10.1016/j.jot.2023.04.003>

Received 30 November 2022; Received in revised form 16 March 2023; Accepted 3 April 2023

The Translational Potential of This Article: This study provides new insights into the use of 1,25(OH)₂D₃ to prevent and treat intervertebral disc degeneration caused by vitamin D deficiency.

1. Introduction

Intervertebral disc degeneration (IVDD) can be affected by a variety of risk factors, which interact with each other and lead to the reduction of the number of intervertebral disc cells, phenotypic transformation, metabolic disorder, decrease of extracellular matrix and imbalance of the microenvironment through different mechanisms [1]. Thereafter, the structural integrity of the intervertebral disc is lost and intervertebral disc degeneration is further accelerated. However, a research gap remains in understanding the pathogenesis and etiology of IVDD.

It has been reported that vitamin D is closely associated with rickets [2], osteoarthritis [3], osteoporosis [4] and lumbar disc herniation [5,6]. The vitamin D receptor (VDR) is widely expressed in intervertebral disc cells, and in various studies, genetic polymorphisms, such as TaqI (rs731236), FokI (rs2228570), and ApaI (rs7975232), have been implicated in the pathogenesis of IVDD [7,8]. The association between vitamin D and degenerative disc disease is strong, as it has been demonstrated in large groups with diverse ethnic backgrounds, including Australian, British, Chinese, Japanese and Finnish populations [9]. Previous studies have shown that vitamin D regulates proliferation of nucleus pulposus (NP) and annulus fibrosus cells, the expression of extracellular matrix genes, synthesis of structural proteins, cytokines, and growth factors [10, 11]. To date, however, no studies have been reported on intervertebral disc degeneration caused by vitamin D deficiency. We previously established a 1,25-dihydroxyvitamin D (1,25(OH)₂D)-deficient mouse model by knocking out the Cyp27b1 (1 α (OH)ase) [1 α (OH)ase^{+/-}] gene [12] as well as other genetically modified models. Phenotypic analysis of these models demonstrated the role and mechanism of 1,25(OH)₂D in delaying aging and associated diseases [13–22]. However, it is unknown whether 1, 25(OH)₂D deficiency can induce intervertebral disc degeneration *in vivo*.

Sirt1 is a nicotinamide adenine dinucleotide (NAD⁺)-dependent deacetylase and is considered as a longevity gene [23]. Recent study indicate that Sirt1 is a protective mediator in IVDD and the expression of Sirt1 decreases in degenerative disc [24]. The Sirt1 activator resveratrol protects against intervertebral disc injury by regulating cellular senescence and promoting regeneration, whereas Sirt1 deficiency worsens intervertebral disc degeneration after needle puncture [25]. To investigate the role in osteogenesis of Sirt1 in MSCs, we constructed a transgenic mouse model by overexpressing Sirt1 in MSCs using Prx1 as a promoter (Sirt1^{Tg}) [26,27]. The transcription factor Prx1, a marker of MSCs, is widely used for mesenchymal lineage-specific knockdown or overexpression of target genes, and MSCs can differentiate into NP-like cells [28]. Results from our studies showed that overexpression of Sirt1 in MSCs protected against bone loss induced by Bmi1 or 1,25(OH)₂D deficiency in long bone or mandibles [26,27,29]. However, it is unclear whether overexpression of Sirt1 in MSCs protects against IVDD induced by 1,25(OH)₂D deficiency.

In this study, we compared the phenotypes of intervertebral discs between wild-type and 1 α (OH)ase^{+/-} mice at 8 months of age to determine whether 1,25(OH)₂D insufficiency plays a role in promoting intervertebral disc degeneration *in vivo*. Then we used Prx1-driven Sirt1 transgenic mice (Sirt1^{Tg}) and generated a mouse model that overexpressed Sirt1 in MSCs on a 1 α (OH)ase^{+/-} background (Sirt1^{Tg}1 α (OH)ase^{+/-}) and compared their intervertebral disc phenotypes with those of Sirt1^{Tg}, 1 α (OH)ase^{+/-} and wild-type littermates at 8 months of age. Furthermore, we generated a NP cell model with reduced VDR expression and then treated this model with 1,25(OH)₂D₃, or resveratrol or 1,25(OH)₂D₃ plus Ex527 (an inhibitor of Sirt1), and examined their effects. The results of this study provide novel insight into potential treatments to prevent IVDD caused by 1,25(OH)₂D/VDR deficiency.

2. Materials and methods

2.1. Experimental animals

In this study we used three types of mouse models: (1) Sirt1^{Tg} mice, which were originally generated in our laboratory, and overexpress Sirt1 in mesenchymal lineage cells, driven by the 2.4 kb Prx1 promoter. (2) 1 α (OH)ase^{+/-} mice on a BALB/c background which were backcrossed with wild-type mice on a C57BL/6J background for 12 generations to obtain 1 α (OH)ase^{+/-} mice with C57BL/6J background. (3) Sirt1^{Tg}/1 α (OH)ase^{+/-} mice, which were generated by mating the 1 α (OH)ase^{+/-} mice and Sirt1^{Tg} mice on a C57BL/6J background to produce offspring heterozygous at both loci, which were then mated to generate double heterozygous mice. Eight-month-old male wild-type (WT), Sirt1^{Tg}, 1 α (OH)ase^{+/-}, and Sirt1^{Tg}/1 α (OH)ase^{+/-} littermates were used. All animal experiments were approved by the Institutional Animal Care and Use Committee of Nanjing Medical University.

2.2. Micro-computed tomography (micro-CT)

The vertebral columns of each mouse from L1 to L4 were isolated from the spine and soft-tissue was removed to reduce muscles and ligament interference. A micro-CT scanner (Skyscan, 1176) was used to evaluate the spine samples. The scans were performed using the following scanner settings: voltage 45 kV, current 500 μ A and a 780 ms integration time. The resolution of the computed image is 2672 \times 4000 and the slice thickness is 9 μ m. The cross-sectional images were reconstructed to three-dimensional diagrams and analyzed using a CT-Analyzer (SkyScan-10) analysis program. The invisible area between the distal endplate of L1 and the proximal endplate of L2 was defined as the region of interest (ROI) of intervertebral disc analysis. The height of intervertebral disc was the mean at the ventral, midline and dorsal areas along the midsagittal plane. The intervertebral disc volume was quantitatively analyzed by three-dimensional reconstruction using 5 consecutive ROI coronal plane images.

2.3. Immunohistochemistry and histopathologic analyses

The disc specimens were fixed with formaldehyde, embedded in paraffin, and then cut serially into 5- μ m sections. The sections were deparaffinized, rehydrated, and subjected to stain with HE and Safranin-O and immunohistochemically. The images were then captured by a microscope and evaluated by histology researchers in a blinded manner. For immunohistochemistry, 0.01M sodium citrate was used for antigen retrieval and sections were then incubated with methanol: hydrogen peroxide (1:10) to block endogenous peroxidase activity and then washed in Tris-buffered saline, blocked with 5% normal goat serum. The slides were then incubated at 4 °C overnight with the primary antibodies against aggrecan (1:100 dilution; Wanleibio, China), type 2 collagen (COL2, 1:100 dilution; Wanleibio, China), MMP13 (1:100 dilution; Proteintech, USA), TNF- α (1:100 dilution; Proteintech, USA), IL-1 β (1:100 dilution; Wanleibio, China), p65 (1:100 dilution; Abmart, China), and Sirt1 (1:100 dilution; Proteintech, USA). Then, the sections were incubated with secondary antibodies. Sections were then washed and incubated with the Vectastain Elite ABC reagent (Vector Laboratories) for 30 min. Staining was done using 3,3'-diaminobenzidine (2.5 mg/mL) followed by counterstaining with Mayer's hematoxylin. The images were quantified using IMAGE J software to determine the percentages of positive cells in the samples.

2.4. Western blotting

Intervertebral disc tissue or NP cells were lysed by using RIPA lysis buffer (Beyotime, China) with 1% PI on ice. The protein concentration was determined by using a bicinchoninic acid (BCA) assay (Beyotime, China). 30 µg proteins of each sample were electrophoresed by performing sodium dodecylsulphate polyacrylamide gel electrophoresis (SDS-PAGE) on 10% gels. The separated proteins were transferred onto a PVDF membrane and blocked with 5% bovine serum albumin (BSA, gibco, USA). Then the membranes were incubated overnight at 4 °C with primary antibodies against aggrecan (1:1000 dilution; Wanleibio, China), COL2 (1:1000 dilution; Wanleibio, China), MMP13 (1:1000 dilution; Proteintech, USA), TNF-α (1:1000 dilution; Proteintech, USA), IL-1β (1:1000 dilution; Wanleibio, China), p65 (1:1000 dilution; Abmart, China), p-p65 (Ser536) (1:1000 dilution; Abcam, UK), acetyl-p65 (Lys310) (1:1000 dilution; Abcam, UK), Sirt1 (1:1000 dilution; Proteintech, USA), Prx-1(1:1000 dilution; Proteintech, USA) and β-actin (1:10000 dilution; Proteintech, USA). Finally, the membranes were washed and incubated with HRP-conjugated secondary antibody (1:5000 dilution; Beyotime, China) at room temperature for 2 h. Immunoreactive bands were visualized with ECL chemiluminescence (ChemiDoc XRS+, Bio-Rad, USA) and analyzed by Image lab.

2.5. Real-time reverse transcription polymerase chain reaction (RT-PCR)

Total RNA was extracted from IVD or NP cells by using RNAiso Plus (Beyotime, China) according to the manufacturer's instructions. The cDNA was synthesized using Synthesis SuperMix (Vazyme, China). Then the cDNA samples were amplified by performing real-time RT-PCR in Agilent Real-time System by using SYBR® Green Real-Time PCR Master Mix (Vazyme, China). The PCR reaction protocol was as follows: 95 °C for 30s, followed by 40 cycles at 95 °C for 5s, 60 °C for 30s then annealing and extension at 95 °C for 15s, 60 °C for 60s and 95 °C for 15s. All relative mRNA expression levels were calculated by normalized endogenous GAPDH, according to the 2-ΔΔCt method. The primer sequences used for the real-time PCR are displayed in Table 1.

2.6. Isolation and culture of mouse nucleus pulposus cells

NP cells were isolated from lumbar discs of 5 mice on a C57BL/6J background as described previously [30]. Briefly, the spinal columns of mice (8 weeks old) were removed whole under aseptic conditions and

lumbar intervertebral discs were collected. The gel-like NP was isolated from the annulus fibrosus under a microscope and treated with 0.1% type II collagenase (Beyotime, China) and 2 U/mL hyaluronidase (Beyotime, China) for 2 h at 37 °C to digest the tissue completely. After centrifugation at 1500 rpm for 5 min, the precipitates were resuspended and placed in high glucose DMEM/F-12 (Beyotime, China) medium containing 10% FBS and 1% penicillin/streptomycin antibiotics in an incubator maintained with 5% CO₂ at 37 °C. The complete medium was replaced every other day. When confluent, the NP cells were harvested using trypsin-EDTA (1 mM, gibco, USA) solution and subcultured into suitable petri dish for later use.

2.7. Ad-siVDR transfection

The adenovirus (RNA interference) containing siRNA against VDR (Ad-siVDR) was synthesized and a GV161 plasmid was generated using the AdMax system (Genechem Co., Ltd, China) according to the manufacturer's protocols. A scrambled sequence (200 µL; Genechem Co., Ltd, China) was used as the negative control (NC). NP cells were seeded and incubated at 37°C for 24 h in a medium dish. When NP cells reached 50% confluency, they were incubated with Ad-siVDR or Ad-NC at a multiplicity of infection (MOI) of 1000 at 37 °C with 5% CO₂. At 12 h post-inoculation, the medium containing adenovirus was removed and replaced with complete medium. 48 h later, the cells were observed using phase contrast fluorescence microscope (Leica DM4000BLED, Germany). The transfection efficiency of Ad-siVDR was assessed by Real-time PCR (RT-PCR) to evaluate the gene expression level and Western blotting to examine the protein expression level.

2.8. Cell treatment

Six groups of NP cells were designated: 1) Control: NP cells incubated in complete medium; 2) NC: Scrambled negative control adenovirus transfected NP cells incubated in complete medium; 3) Ad-siVDR: The adenovirus (RNA interference) containing siRNA against VDR transfected NP cells incubated in complete medium; 4) Ad-siVDR + VD: Cells were transfected with Ad-siVDR for 12 h before the addition of 10⁻⁸ M 1,25(OH)₂D₃; 5) Ad-siVDR + VD + Ex527: Cells were transfected with Ad-siVDR for 12 h before the addition of 10⁻⁸ M 1,25(OH)₂D₃ and 10 µM Sirt1 inhibitor Ex527; 6) Ad-siVDR + RES: Cells were transfected with Ad-siVDR for 12 h before the addition of 100 µM resveratrol.

2.9. Immunofluorescence (IF) staining

The treated NP cells were fixed with 4% paraformaldehyde for 30 min and permeabilized with 0.5% Triton-X for 20min. Then, the cells were blocked with 5% bovine serum albumin (BSA) for the preparation of IF staining. Following, the cells were incubated with primary antibody against Sirt1 (1:100 dilution; Proteintech, USA), p16 (1:1000 dilution; Abcam, UK), aggrecan (1:100 dilution; Wanleibio, China), COL2 (1:100 dilution; Wanleibio, China), MMP13 (1:100 dilution; Proteintech, USA), tumor necrosis factor-α (TNF-α) (1:100 dilution; Proteintech, USA), interleukin 1β (IL-1β) (1:100 dilution; Wanleibio, China), p65 (1:100 dilution; Abmart, China) overnight at 4 °C. The next day after washing, NP cells were incubated with Alexa Fluor488 secondary antibody (Invitrogen, Carlsbad, CA, USA) at room temperature for 1 h, followed by staining nucleus with 4',6-diamidino-2- phenylindole (DAPI) for 5min. Each step was followed by washing with PBS. The staining intensity of the fluorescence was represented the expression of proteins. For 5-ethynyl-2'- deoxyuridine (EdU) assay to evaluate cell proliferation, cultured NP cells were incubated with EdU for 2 h, after which EdU staining was performed using Apollo567 Stain Kit (RiboBio) according to the manufacturer's instructions. Immunofluorescence double staining for p16 and p65 were also performed in the paraffin sections of intervertebral disc tissue.

Table 1

Primers used in this study for real time RT-PCR.

Gene	Primer Sequence	Species
GAPDH	Forward: 5'- GCACCGTCAAGGCTGAGAAC-3'	mouse
	Reverse:5'- TGGTGAAGACGCCAGTGA-3'	
MMP3	Forward: 5'- GTCCCTCTATGGAATCCAC-3'	mouse
	Reverse:5'- AGTCCTGAGAGATTTGCGCC-3'	
MMP13	Forward: 5'- TGTTTCAGAGCACTACTTGAA-3'	mouse
	Reverse:5'- CAGTCACCTTAAGCCAAAGAAA-3'	
Col-2	Forward: 5'- GGAATGTCTCTCGATGAC-3'	mouse
	Reverse:5'- GAAGGGGATCTCGGGTTG-3'	
Aggrecan	Forward: 5'- CTACCAGTGGATCGGCCTGAA-3'	mouse
	Reverse:5'- CGTGCCAGATCATACCACA-3'	
Sirt1	Forward: 5'- GGTGACGACTTCGACGACG-3'	mouse
	Reverse:5'- TCGGTCAACAGGAGTTGTCT-3'	
Prx-1	Forward: 5'- AATGCAAAAATTGGGTATCCTGC-3'	mouse
	Reverse:5'- CGTGGGACACAAAAGTAAAGT-3'	
TNF-α	Forward: 5'- TCTACTGAACTTCGGGGTGATCG-3'	mouse
	Reverse:5'- AGATGATCTGAGTGTGAGGGTCTGG-3'	
IL-1β	Forward: 5'- GCTGAAAGCTCTCCACCTCAATG-3'	mouse
	Reverse:5'- TGTCGTTGCTGGTCTCCTTG-3'	
p65	Forward: 5'- AGGCTTCTGGCCCTATGTG-3'	mouse
	Reverse:5'- TGCTTCTCTCGCCAGGAATAC-3'	
VDR	Forward: 5'- ACCCTGGTGACTTTGACCG-3'	mouse
	Reverse:5'- GGCAATCTCCATTGAAGGGG-3'	

2.10. SA-β-gal cytochemical and p16 immunocytochemical double staining

For senescence-associated β-galactosidase (SA-β-Gal) stain, cells were fixed with 2% formaldehyde combined with 0.25 glutaraldehyde for 5 min, followed by the introduction of 1 mL SA-β-Gal dye (Beyotime, China) for 2 h at 37 °C, blue precipitation was observed, subsequently, immunocytochemical staining for p16 was performed.

2.11. Co-immunoprecipitation assay

The interaction between Sirt1 and NFκB was detected by protein A/G magnetic beads immunoprecipitation assay (Thermo Fisher Scientific Inc, USA), according to the manufacturer's instructions. Firstly, anti-Sirt1 antibody was added to 50 μg of the protein sample and incubated at 37 °C

for 1 h. Then the protein-A/G beads were mixed with the sample and incubated overnight in a shaker at 4 °C. The next day, the beads were resuspended in lysis buffer and the bound antigens were eluted from the beads with sodium dodecyl sulfate sample buffer. The proteins were then analyzed by performing Western blotting with anti-p65 antibody.

Whole cell and nuclear extracts were prepared for Western blot analysis. NP cells were collected in 1.5 mL tube. Pelleted cells were resuspended in 150 μL ice-cold buffer A with 2 μL protease inhibitors and 2 μL phosphatase inhibitors (BestBio, China) for 30 min on ice and vortexed for 10 s every 10 min. After centrifugation (7000 rpm 3 min 4 °C) the supernatant was collected and stored at -20 °C (cytoplasmic protein fraction). Then 150 μL of extracting solution B with 1 μL protease inhibitors and 1 μL phosphatase inhibitors (BestBio, China) and 5 μL extracting solution C were added to the pellet for 30 min on ice and

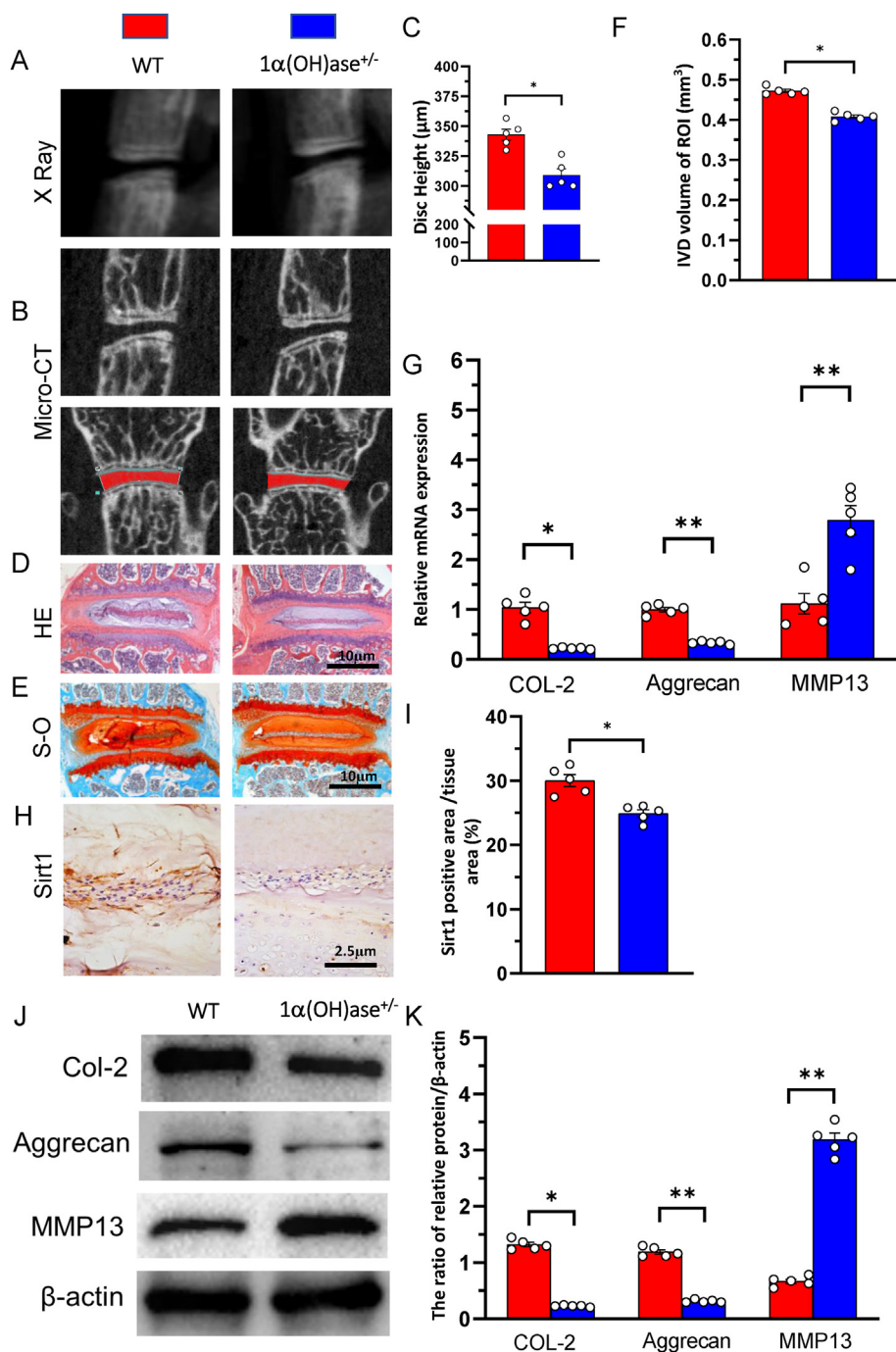


Figure 1. 1,25(OH)₂D₃ deficiency accelerated intervertebral disc degeneration (A) Representative radiographs and (B) images of micro-CT-scanned sagittal plane and coronal plane of L1/2 segment from 8-month-old wild-type (WT) and 1α(OH)ase^{+/-} mice (C) Disc height of L1/2 in wild-type (WT), 1α(OH)ase^{+/-} mice. Representative micrographs of decalcified paraffin-embedded sections through the intervertebral disc from 8-month-old WT, and 1α(OH)ase[±] mice were stained with (D) hematoxylin and eosin (HE) (E) Safranin O-Fast Green (S-O) and (H) immunohistochemically for Sirt1 (F) Intervertebral disc volume of L1/2 in WT and 1α(OH)ase^{+/-} mice (G) Real-time RT-PCR of tissue extracts of intervertebral discs for expression of Col-2, aggrecan and MMP13. Messenger RNA expression assessed by real-time RT-PCR is calculated as a ratio relative to GAPDH, and expressed relative to WT mice (I) The percentages of Sirt1 positive area (J) Western blots of intervertebral disc extracts were carried out for the expression of Col-2, aggrecan and MMP13 (K) Protein levels relative to β-actin were assessed by densitometric analysis, and expressed relative to WT mice. Values are mean ± S.E.M. of 5 determinations per group. The differences between the two groups were analyzed by using the Student's t-test. *: P < 0.05 **: P < 0.01, ***: P < 0.001. (For interpretation of the references to colour in this figure legend, the reader is referred to the Web version of this article.)

vortexed for 10 s every 10 min. After centrifugation (7000 rpm, 3 min, 4 °C) the supernatant was collected and stored at –20 °C (nuclear protein fraction). The proteins were then analyzed by performing Western blotting with anti-p65 (1:1000 dilution; Abmart, China) and anti-ace p65 antibody (1:1000 dilution; Abcam, UK).

2.12. Statistical analysis

Data analysis was performed using SPSS 22.0 (IBM Corp. Armonk, N.Y.), and the results which were normally distributed were presented as mean \pm S.E.M. The differences between the two groups were analyzed by using the Student's t-test. A comparison between multiple groups was assessed by using one-way ANOVA test followed by Post-Hoc Test (Least Significant Difference). $P < 0.05$ was considered a statistically significant difference between groups.

3. Results

3.1. 1,25(OH)₂D insufficiency accelerated intervertebral disc degeneration

To investigate whether 1,25(OH)₂D insufficiency plays a role in promoting intervertebral disc degeneration in vivo, the phenotypes of intervertebral discs were compared between wild-type and 1 α (OH)ase^{+/-} mice at 8 months of age using iconography, histology, and molecular biology. The results showed that the intervertebral disc height and volume, the expression of type II collagen and aggrecan at both mRNA and protein levels were significantly decreased, whereas the expression of MMP13 at both mRNA and protein levels was dramatically up-regulated in intervertebral disc regions of interest of 1 α (OH)ase^{+/-} mice compared with those of wild-type littermates (Fig. 1A–G, J & K). We also examined Sirt1 expression in intervertebral discs using immunostaining and found that Sirt1 positive product was detected in NP tissues and the percentage of Sirt1 positive area was significantly decreased in 1 α (OH)ase^{+/-} mice compared with WT mice (Fig. 1H and I). These results demonstrated that 1,25(OH)₂D insufficiency accelerated intervertebral disc degeneration by reducing extracellular matrix protein synthesis and enhancing extracellular matrix protein degradation with reduced Sirt1 expression in NP tissues.

3.2. Overexpression of Sirt1 in MSCs prevents 1,25(OH)₂D insufficiency-induced intervertebral disc degeneration

To determine whether 1,25(OH)₂D₃ prevents intervertebral disc degeneration via Sirt1 in vivo, we used Prx1-driven Sirt1 transgenic mice (Sirt1^{Tg}) and generated a mouse model that overexpressed Sirt1 in MSCs on a 1 α (OH)ase^{+/-} background (Sirt1^{Tg}/1 α (OH)ase^{+/-}). We then compared their intervertebral disc phenotypes with those of Sirt1^{Tg}, 1 α (OH)ase^{+/-} and wild-type littermates at 8 months of age using iconography, histology and molecular biology. The results showed that the intervertebral disc height and volume, the percentages of Sirt1, type II collagen and aggrecan positive areas, the expression of Prx1, Sirt1, type II collagen and aggrecan at both mRNA and protein levels were significantly increased in Sirt1^{Tg} mice, and significantly decreased in 1 α (OH)ase^{+/-} mice relative to wild-type mice; these parameters were significantly increased in Sirt1^{Tg}/1 α (OH)ase^{+/-} mice relative to 1 α (OH)ase^{+/-} mice (Fig. 2A–M, P & Q). In contrast, the percentages of MMP13 positive areas and the expression of Mmp3 and 13 at both mRNA and protein levels were insignificantly decreased in Sirt1^{Tg} mice, but dramatically increased in 1 α (OH)ase^{+/-} mice relative to wild-type mice; these parameters were significantly increased in Sirt1^{Tg}/1 α (OH)ase^{+/-} mice relative to 1 α (OH)ase^{+/-} mice (Fig. 1N–Q). These results demonstrated that overexpression of Sirt1 in MSCs protected against 1,25(OH)₂D insufficiency-induced intervertebral disc degeneration.

3.3. Overexpression of Sirt1 in MSCs prevents 1,25(OH)₂D insufficiency-induced intervertebral disc degeneration by inhibiting the NF- κ B inflammatory pathway

To determine whether the 1,25(OH)₂D insufficiency-induced intervertebral disc degeneration prevented by overexpression of Sirt1 in MSCs was associated with inhibiting the nuclear factor kappa-B (NF- κ B) inflammatory pathway, we examined the expression levels of NF- κ B inflammatory pathway related molecules in NP tissue using immunofluorescence for p16/p65 double staining, immunohistochemical staining for TNF- α and IL-1 β , Western blots and real-time RT-PCR. The results showed that the percentages of p16 and p65 single positive cells, and p16/p65 double positive cells, and the percentages of TNF- α and IL-1 β positive areas, the protein expression levels of ace-p65 and p-p65 and total p65, ratios of ace-p65/p-p65 and p-p65/p65, and the protein and mRNA expression levels of TNF- α and IL-1 β were all significantly increased in 1 α (OH)ase^{+/-} mice relative to wild-type littermates, whereas all above parameters were significantly decreased in Sirt1^{Tg}/1 α (OH)ase^{+/-} mice relative to 1 α (OH)ase^{+/-} littermates (Fig. 3A–K). These results indicate that 1,25(OH)₂D insufficiency induced intervertebral disc degeneration by increasing acetylation and phosphorylation of p65 and activating the NF- κ B inflammatory pathway; in contrast, overexpression of Sirt1 in MSCs prevented 1,25(OH)₂D insufficiency-induced intervertebral disc degeneration by decreasing acetylation and phosphorylation of p65 and inhibiting the NF- κ B inflammatory pathway.

3.4. VDR or resveratrol activates Sirt1 to deacetylate p65 and inhibit its activity in nucleus pulposus cells

Our previous study demonstrated that 1,25(OH)₂D₃ upregulated Sirt1 expression via VDR-mediated transcription and resveratrol also upregulated Sirt1 expression (Chen Haiyun, 2020). To determine whether VDR or resveratrol activates Sirt1 to deacetylate p65 and inhibit its activity in NP cells, we generated a VDR-deficient cellular model by knocking down endogenous VDR using Ad-siVDR transfection into NP cells; in these cells, mRNA and protein expression levels of VDR were markedly decreased in Ad-siVDR transfected NP cells relative to control cells (Fig. 4A–C). Nevertheless, about 30% of the original VDR was still expressed in NP cells after VDR knock-down (Fig. 4A–C). Then, VDR-deficient NP cells were treated with or without resveratrol, and the interactions between Sirt1 and acetylated p65 level and p65 nuclear localization were examined using co-immunoprecipitation, Western blots and immunofluorescence staining. The results showed that total Sirt1 level was downregulated and total p65 level was up-regulated and the ratio of acetylated p65/p65 bound to Sirt1 was significantly higher in VDR knocked down NP cells relative to the control cells, whereas these alterations were largely rescued in resveratrol-treated VDR knocked down NP cells (Fig. 4D and E). Sirt1 levels in the nucleus were downregulated, p65 levels in the nucleus and p65 nuclear localization were increased in VDR knocked down NP cells relative to the control cells, whereas these alterations were largely rescued in resveratrol-treated VDR knocked down NP cells (Fig. 4F and G). These results indicate that VDR or resveratrol activates Sirt1 to deacetylate p65 and inhibit its nuclear translocation in NP cells.

3.5. 1,25(OH)₂D₃/VDR mediated via Sirt1 stimulates the proliferation and inhibits senescence of nucleus pulposus cells

To determine whether 1,25(OH)₂D₃/VDR mediated via Sirt1 stimulates the proliferation and inhibits senescence of NP cells, VDR-deficient NP cells were treated with 1,25(OH)₂D₃, or resveratrol or 1,25(OH)₂D₃ plus Ex527 (an inhibitor of Sirt1); we then examined the alterations of Sirt1 mRNA and protein expression, EdU and p16 positive cells and p16/

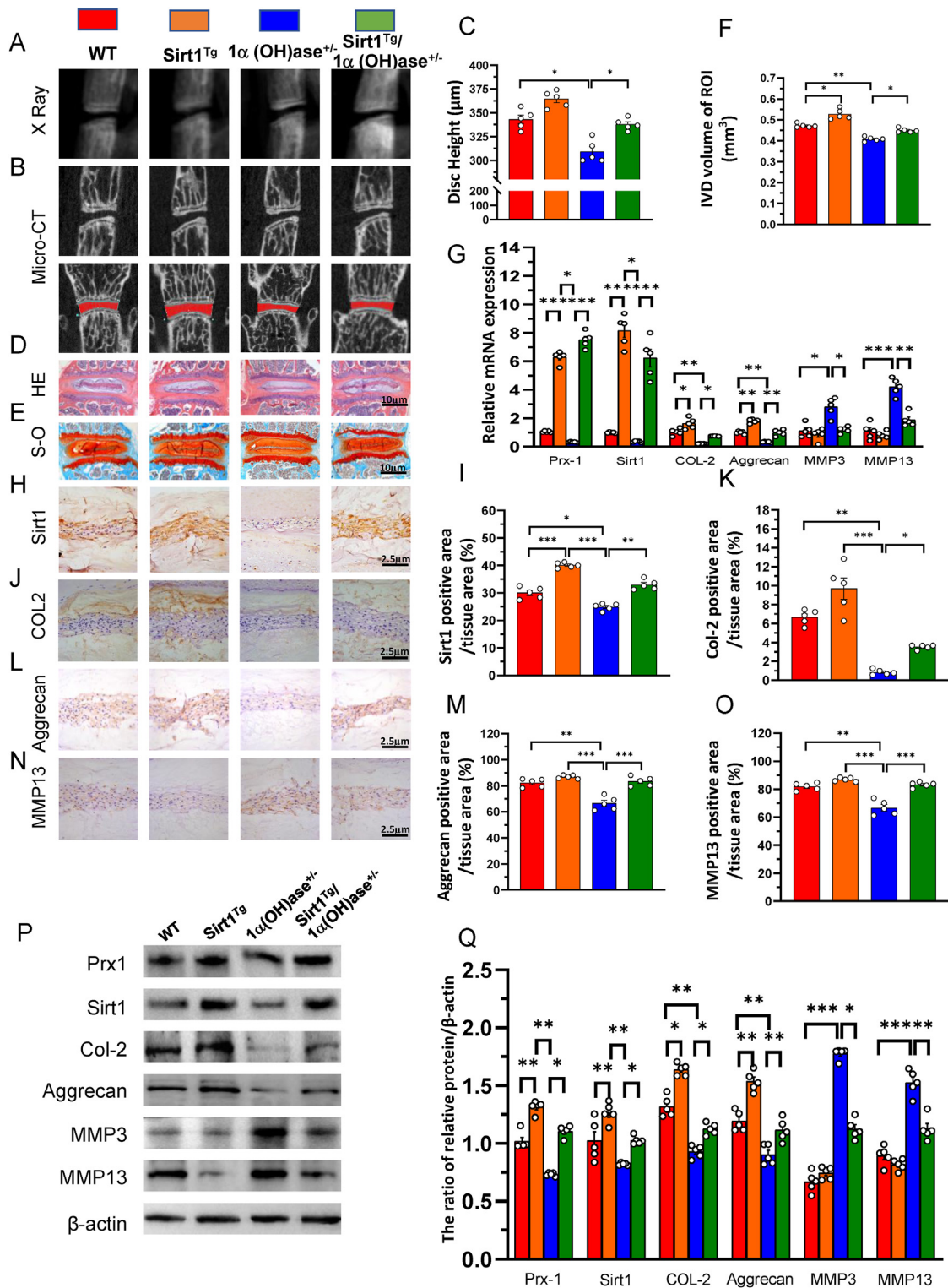


Figure 2. Overexpression of Sirt1 in NP tissues prevents 1,25(OH)₂D₃ deficiency-induced intervertebral disc degeneration (A) Representative radiographs and (B) images of micro-CT-scanned sagittal plane and coronal plane of L1/2 segment from 8-month-old WT, Sirt1^{Tg}, 1 α (OH)ase^{+/-} and Sirt1^{Tg}/1 α (OH)ase^{+/-} mice (C) Disc height of L1/2 in WT, Sirt1^{Tg}, 1 α (OH)ase^{+/-} and Sirt1^{Tg}/1 α (OH)ase^{+/-} mice. Representative micrographs of decalcified paraffin-embedded sections through the intervertebral disc from 8-month-old mice were stained with (D) hematoxylin and eosin (HE) (E) Safranin O-Fast Green (S-O) and immunohistochemically for (H) Sirt1 (J) Col-2 (L) aggrecan and (N) MMP13 (F) Intervertebral disc volume of L1/2 in above 4 genotype mice (G) Real-time RT-PCR of tissue extracts of intervertebral discs for expression of *Prx-1*, *Sirt1*, *Col-2*, *aggrecan*, *MMP3* and *MMP13*. Messenger RNA expression assessed by real-time RT-PCR is calculated as a ratio relative to GAPDH, and expressed relative to WT mice. The percentages of (I) Sirt1 positive area (K) Col-2 positive area (M) aggrecan positive area and (O) MMP13 positive area (P) Western blots of intervertebral disc extracts were carried out for expression of Prx-1, Sirt1, Col-2, aggrecan, MMP3 and MMP13 (Q) Protein levels relative to β -actin were assessed by densitometric analysis. Values are mean \pm S.E.M. of 5 determinations per group. A comparison between multiple groups was assessed by using one-way ANOVA test followed by Post-Hoc Test (Least Significant Difference). *: P < 0.05 **: P < 0.01, ***: P < 0.001. (For interpretation of the references to colour in this figure legend, the reader is referred to the Web version of this article.)

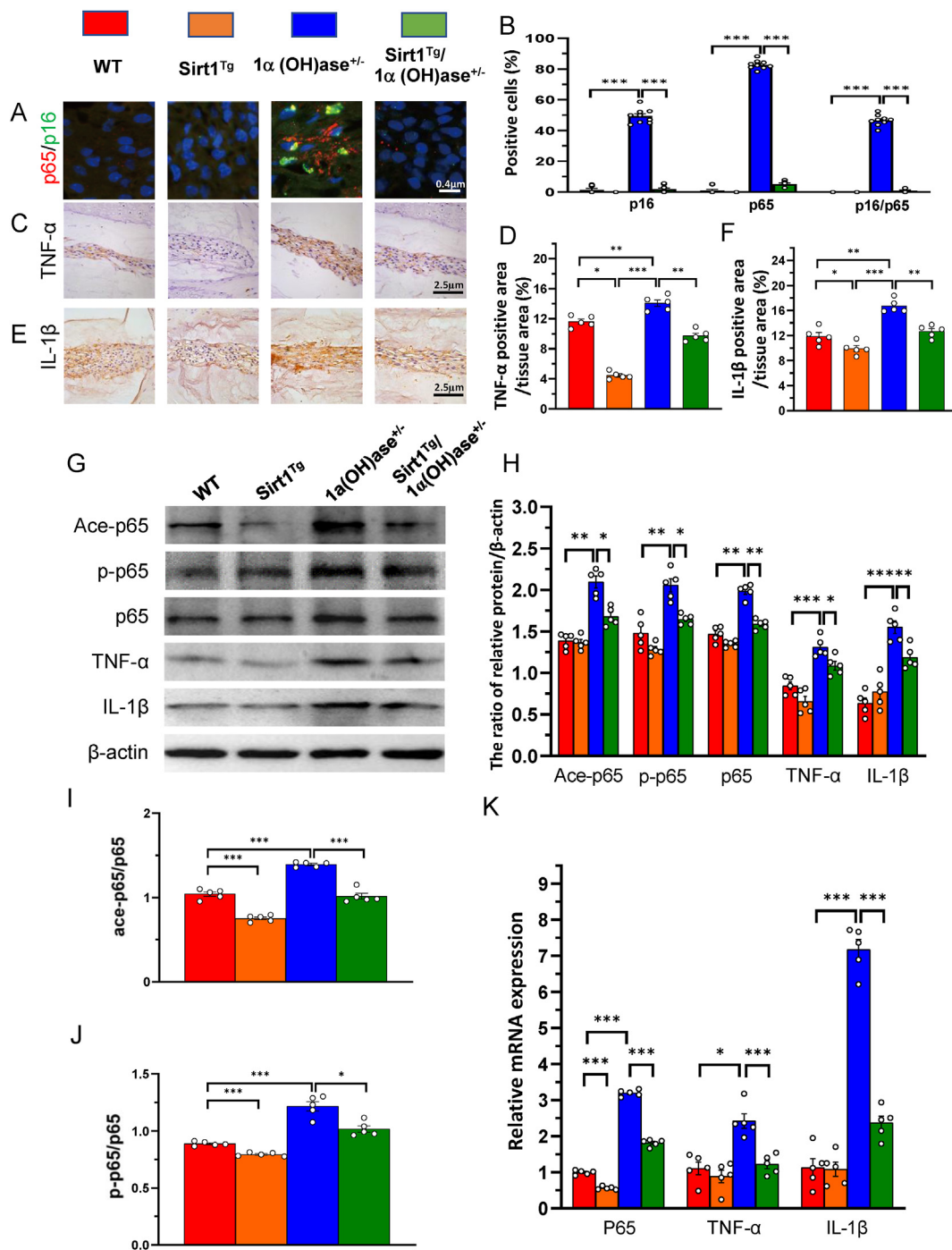


Figure 3. Sirt1 prevents 1,25(OH)₂D₃ deficiency-induced intervertebral disc degeneration by inhibiting inflammation mediated by the NF-κB pathway. Representative micrographs of decalcified paraffin-embedded sections through the intervertebral discs from 8-month-old WT, Sirt1^{Tg}, 1α(OH)ase^{+/-} and Sirt1^{Tg}/1α(OH)ase^{+/-} mice were stained with double immunofluorescence for (A) p16 and p65, and immunohistochemically for (C) TNF-α and (E) IL-1β. The percentages of (B) p16 and p65 single positive cells and p16/p65 double positive cells (D) TNF-α positive area and (F) IL-1β positive area (G) Western blots of intervertebral disc extracts were carried out for expression of Ace-p65, p-p65, p65, TNF-α, and IL-1β (H) Protein levels relative to β-actin were assessed by densitometric analysis. Protein levels of (I) Ace-p65 and (J) p-p65 relative to p65 were assessed by densitometric analysis (K) Real-time RT-PCR of tissue extracts of intervertebral discs for expression of p65, TNF-α, and IL-1β. Messenger RNA expression assessed by real-time RT-PCR is calculated as a ratio relative to GAPDH, and expressed relative to WT mice. Values are mean ± S.E.M. of 5 determinations per group. A comparison between multiple groups was assessed by using one-way ANOVA test followed by Post-Hoc Test (Least Significant Difference). *: P < 0.05 **: P < 0.01, ***: P < 0.001.

SA-β-gal double positive cells in NP cells using immunofluorescence staining, SA-β-Gal cytochemical and p16 immunocytochemical double staining, Western blots and real-time RT-PCR. The results showed that the intensity of immunofluorescence staining, mRNA and protein expression levels of Sirt1 and the percentage of EdU positive cells were

significantly reduced in VDR-deficient NP cells relative to control cells. Nevertheless, sufficient VDR was present so that they were partially rescued by the treatment of 1,25(OH)₂D₃ or resveratrol; nevertheless, the partial rescue role with 1,25(OH)₂D₃ was blocked by addition of Sirt1 inhibitor Ex527 (Fig. 5A–D, I & K). Additionally, the percentage of p16

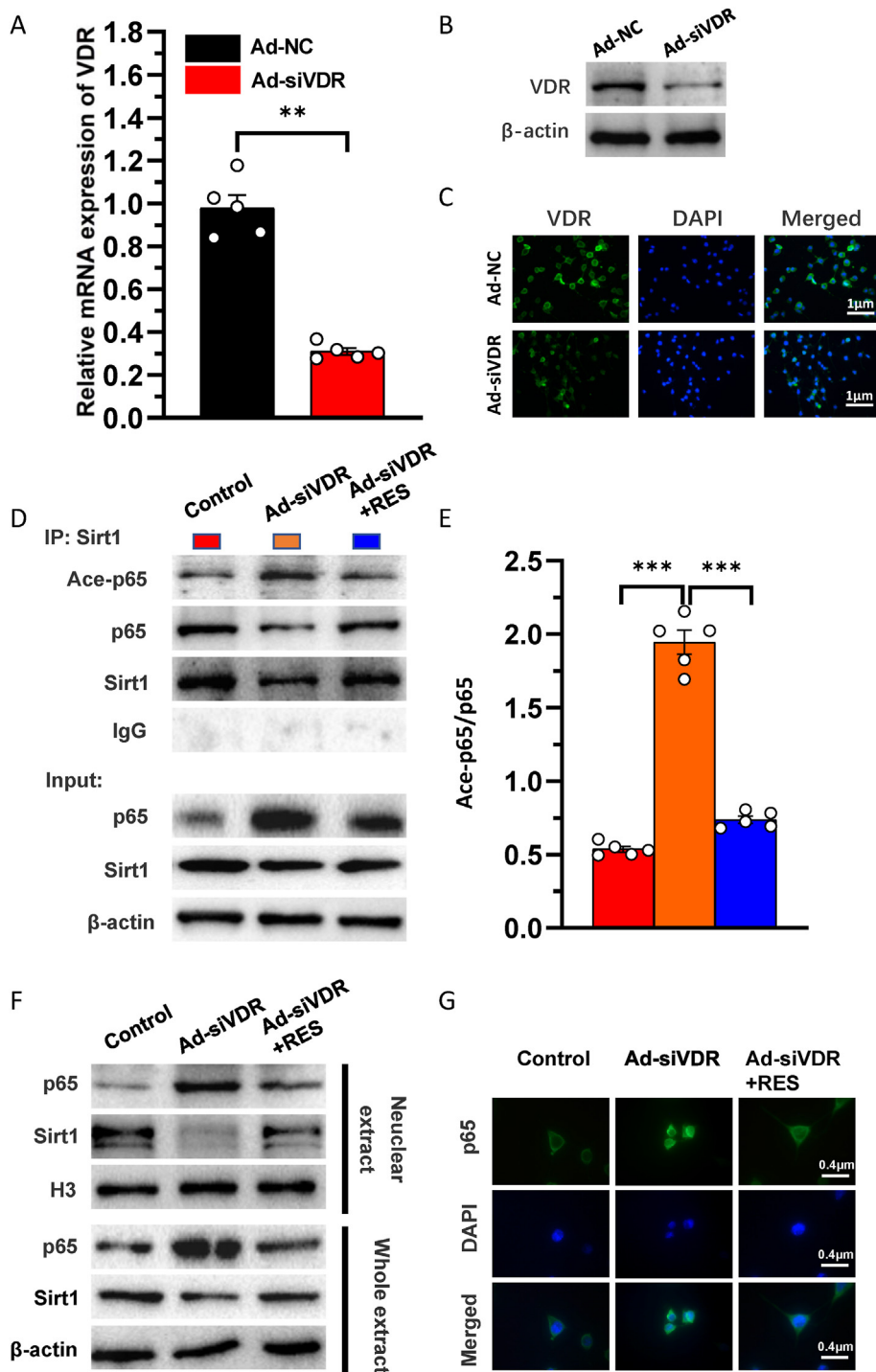


Figure 4. VDR or resveratrol activates Sirt1 to deacetylate p65 and inhibit its activity in nucleus pulposus cells. The knockdown efficiency of VDR by adenovirus vectors transfection with siVDR was detected by (A) real-time RT-PCR for the mRNA level (B) Western blots and (C) immunofluorescence staining for VDR protein expression level. NP cells isolated from intervertebral discs of mice were cultured in blank medium (Control), Ad-siVDR medium and Ad-siVDR with resveratrol (RES) medium (D) Whole cell lysates (WCL) of NP cells were treated with anti-Sirt1 antibody and hybridized with anti-p65 or acetylated p65 antibody. The proteins were then analyzed by performing Western blotting (E) Ace-p65 relative to p65 were assessed by densitometric analysis (F) Whole cell lysates (WCL) and nuclear lysates were blotted with anti-Sirt1 or anti-p65 antibody (G) Representative micrographs of immunofluorescence staining for p65 (green), DAPI (blue) and merge. Values are mean ± S.E.M. of 5 determinations per group. The differences between the two groups were analyzed by using the Student's t-test. A comparison between multiple groups was assessed by using one-way ANOVA test followed by Post-Hoc Test (Least Significant Difference). **: P < 0.01, ***: P < 0.001. (For interpretation of the references to colour in this figure legend, the reader is referred to the Web version of this article.)

positive and p16/SA-β-gal double positive cells were significantly increased in VDR-deficient NP cells relative to control cells, but were partially rescued by treatment with 1,25(OH)₂D₃ or resveratrol; they were significantly increased in VDR-deficient NP cells treated with 1,25(OH)₂D₃ plus Ex527 compared with those treated with 1,25(OH)₂D₃ alone (Fig. 5E–H). These results indicate that 1,25(OH)₂D₃ acting on residual VDR and mediated via Sirt1 stimulates the proliferation and inhibits senescence of NP cells.

3.6. 1,25(OH)₂D₃/VDR mediated via Sirt1 inhibits nucleus pulposus cell degeneration

To determine whether 1,25(OH)₂D₃/VDR mediated via Sirt1 protects against NP cell degeneration, VDR-deficient NP cells were treated as Fig. 5, the alterations of aggrecan and MMP13 mRNA and protein expression were examined in NP cells using real-time RT-PCR, immunofluorescence staining and Western blots. The results showed that the

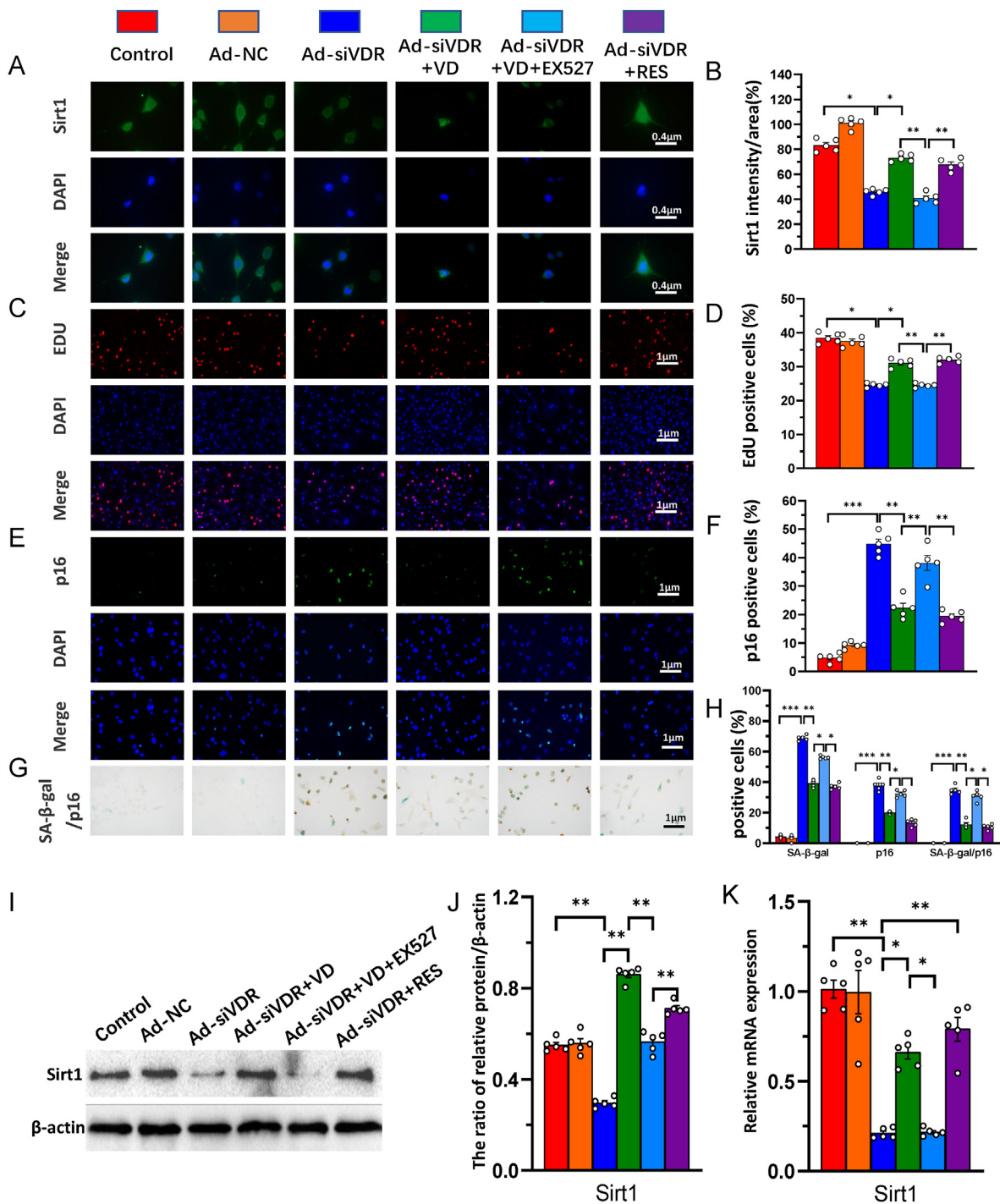


Figure 5. 1,25(OH)₂D₃/VDR mediated via Sirt1 stimulates the proliferation and inhibits senescence of nucleus pulposus cells. NP cells isolated from intervertebral discs of mice were cultured in the absence (Control) or presence of transfected with Ad-NC or Ad-siVDR or Ad-siVDR treated with 10⁻⁸ M 1,25(OH)₂D₃ (VD) or Ad-siVDR treated with 10⁻⁸ M 1,25(OH)₂D₃ and 10 μM Sirt1 inhibitor Ex527 or Ad-siVDR treated with 100 μM resveratrol (Res). Representative micrographs of immunofluorescence staining for (A) Sirt1 (green) (C) EdU (red) (E) p16 (green), DAPI (blue) and merge. The percentages of (B) Sirt1 (D) EdU and (F) p16 positive cells (G) Representative micrographs of cells from SA-β-gal cytochemical and p16 immunocytochemical double staining (H) The percentage of p16, SA-β-gal single positive cells and p16 and SA-β-gal double positive cells (I) Whole cell lysates were blotted with anti-Sirt1 antibody (J) Protein levels relative to β-actin were assessed by densitometric analysis (K) Real-time RT-PCR of NP cell extracts for expression of Sirt1. Messenger RNA expression assessed by real-time RT-PCR is calculated as a ratio relative to GAPDH, and expressed relative to control. Values are mean ± S.E.M. of 5 determinations per group. A comparison between multiple groups was assessed by using one-way ANOVA test followed by Post-Hoc Test (Least Significant Difference). *: P < 0.05 **: P < 0.01, ***: P < 0.001. (For interpretation of the references to colour in this figure legend, the reader is referred to the Web version of this article.)

intensity of immunofluorescence staining, mRNA and protein expression levels of aggrecan were significantly reduced in VDR-deficient NP cells

relative to control cells, they were partially rescued by the treatment of 1,25(OH)₂D₃ or resveratrol, but the partial rescue role of 1,25(OH)₂D₃

was blocked by addition of Sirt1 inhibitor Ex527, whereas the intensity of immunofluorescence staining, mRNA and protein expression levels of MMP13 were significantly increased in VDR-deficient NP cells relative to control cells, they were partially rescued by the treatment of 1,25(OH)₂D₃ or resveratrol, but they were more dramatically increased in VDR-deficient NP cells treated with 1,25(OH)₂D₃ plus Ex527 (Fig. 6A–G). These results indicate that 1,25(OH)₂D₃, binding to residual VDR, and mediated via Sirt1 protects against NP cell degeneration by stimulating extracellular matrix protein synthesis and inhibiting their degradation.

3.7. 1,25(OH)₂D₃/VDR mediated via Sirt1 inhibits NF-κB inflammatory pathway in nucleus pulposus cells

To determine whether 1,25(OH)₂D₃/VDR mediated via Sirt1 inhibits the NF-κB inflammatory pathway, VDR-deficient NP cells were treated as in Fig. 5, and the alterations of the acetylation and phosphorylation levels

of p65, p65, TNF-α and IL-1β protein and mRNA expression were examined in NP cells using immunofluorescence staining, Western blots and real-time RT-PCR. The results showed that the ratio of acetylated and phosphorylated p65/p65, the intensity of immunofluorescence staining, protein and mRNA expression levels of p65, TNF-α and IL-1β were significantly increased in VDR-deficient NP cells relative to control cells, they were partially rescued by the treatment of 1,25(OH)₂D₃ or resveratrol, but the partial rescue role of 1,25(OH)₂D₃ was blocked by addition of Sirt1 inhibitor Ex527 (Fig. 7A–I). These results indicate that 1,25(OH)₂D₃, acting on residual VDR, and mediated via Sirt1 inhibits the NF-κB inflammatory pathway in NP cells.

4. Discussion

It has been demonstrated that vitamin D deficiency is associated with an increased risk of patients developing lumbar disc herniation [5,6]. However, there have not been reports of intervertebral disc degeneration

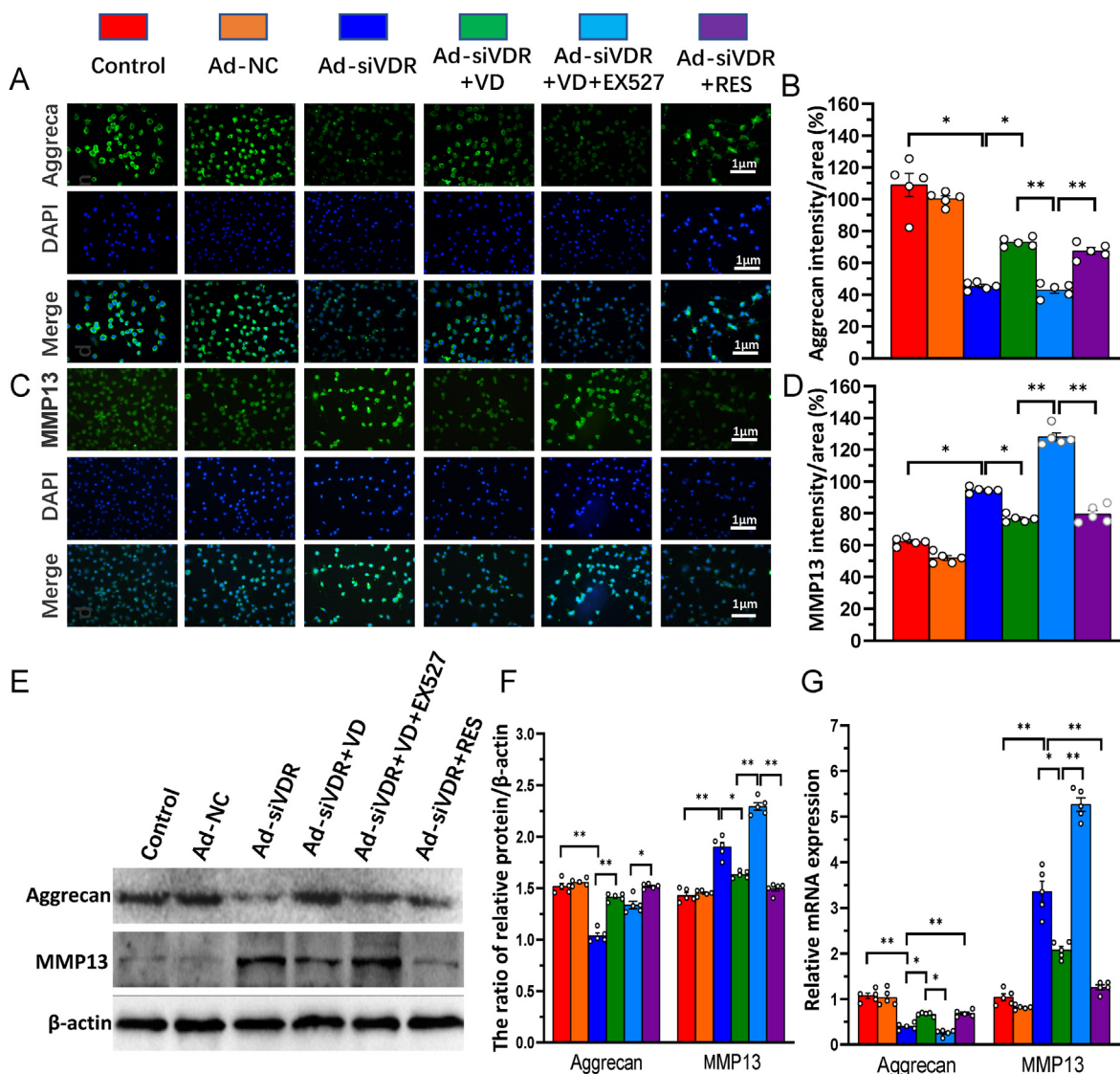
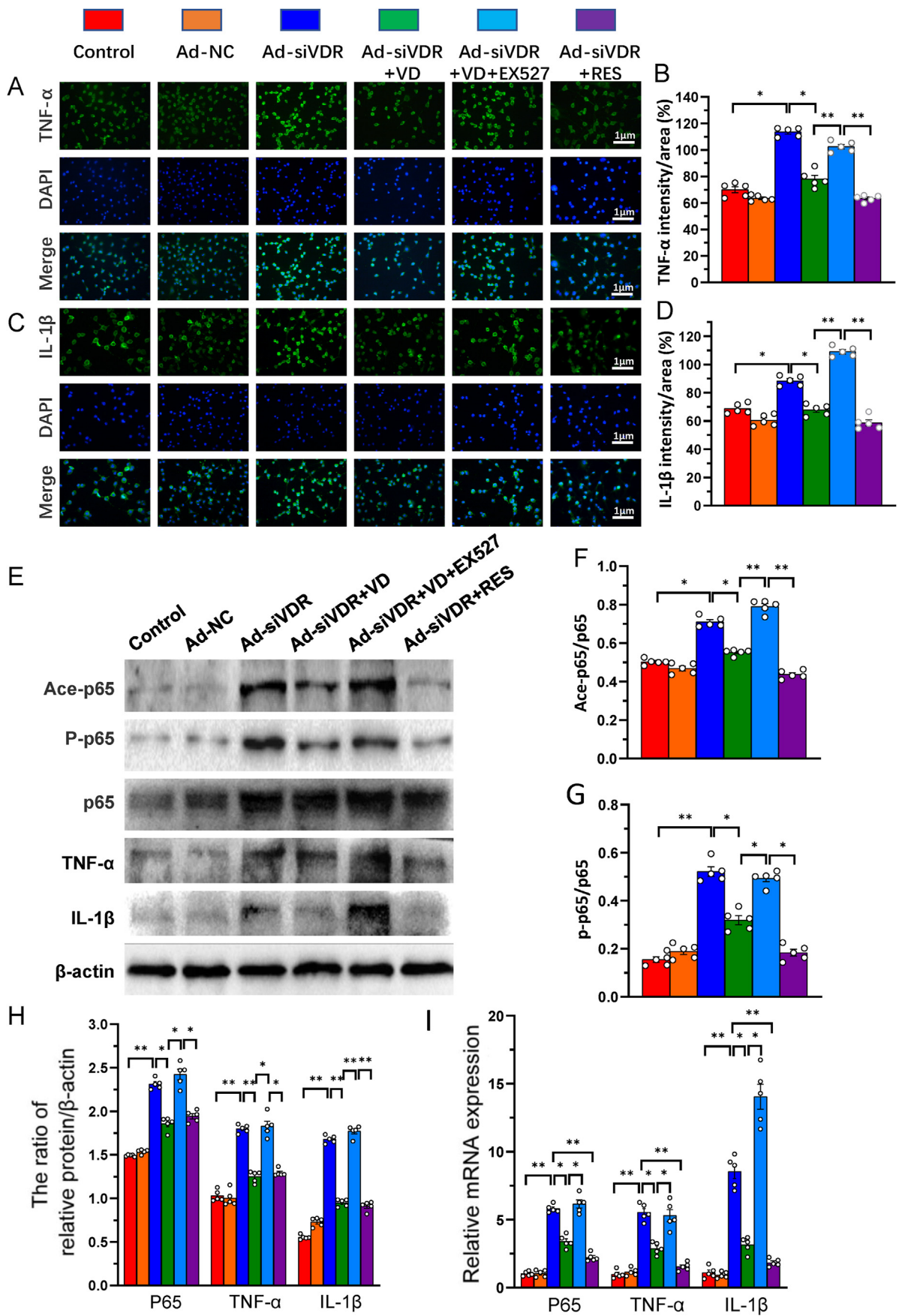


Figure 6. 1,25(OH)₂D₃/VDR mediated via Sirt1 inhibits nucleus pulposus cell degeneration. NP cells isolated from intervertebral discs of mice were cultured and treated as Fig. 5. Representative micrographs of immunofluorescence staining for (A) aggrecan (green) (C) MMP13 (green), DAPI (blue) and merge. The percentages of (B) aggrecan and (D) MMP13 intensity to area (E) Whole cell lysates were blotted with anti-Sirt1 or anti-aggrecan or anti-MMP13 antibody (F) Protein levels relative to β-actin were assessed by densitometric analysis (G) Real-time RT-PCR of NP cell extracts for expression of Sirt1, aggrecan and MMP13. Messenger RNA expression assessed by real-time RT-PCR is calculated as a ratio relative to GAPDH, and expressed relative to control. Values are mean ± S.E.M. of 5 determinations per group. A comparison between multiple groups was assessed by using one-way ANOVA test followed by Post-Hoc Test (Least Significant Difference). *: P < 0.05 **: P < 0.01, ***: P < 0.001. (For interpretation of the references to colour in this figure legend, the reader is referred to the Web version of this article.)



(caption on next page)

Figure 7. 1,25(OH)₂D₃/VDR mediated via Sirt1 inhibits NF-κB inflammatory pathway in nucleus pulposus cells. NP cells isolated from intervertebral discs of mice were cultured and treated as Fig. 5. Representative micrographs of immunofluorescence staining for (A) TNF-α (green) (C) IL-1β (green), DAPI (blue) and merge (B). The percentages of (B) TNF-α and (D) IL-1β intensity to area (E) Whole cell lysates were blotted with anti-Ace-p65, anti-p-p65, anti-p65, anti-TNF-α or anti-IL-1β antibody. Protein levels of (F) Ace-p65 and (G) p-p65 relative to p65 were assessed by densitometric analysis (H) Protein levels relative to β-actin were assessed by densitometric analysis (I) Real-time RT-PCR of NP cell extracts for expression of p65, TNF-α and IL-1β. Messenger RNA expression assessed by real-time RT-PCR is calculated as a ratio relative to GAPDH, and expressed relative to control group. Values are mean ± S.E.M. of 5 determinations per group. A comparison between multiple groups was assessed by using one-way ANOVA test followed by Post-Hoc Test (Least Significant Difference). *: P < 0.05 **: P < 0.01, ***: P < 0.001. (For interpretation of the references to colour in this figure legend, the reader is referred to the Web version of this article.)

caused by vitamin D deficiency. In this study, we compared the phenotypes of intervertebral discs between wild-type and 1α(OH)ase^{+/-} mice at 8 months of age using iconography, histology and molecular biology. Our results demonstrated, for the first time, that 1,25(OH)₂D insufficiency accelerated intervertebral disc degeneration by reducing extracellular matrix protein synthesis and enhancing extracellular matrix protein degradation with reduced Sirt1 expression in NP tissues. Evidence from in vitro and in vivo studies in animals, and from human studies support the concept that IVDD is a common degenerative disease of the musculoskeletal system that develops with age [31]. Our previous studies have shown several age-related diseases in mice with insufficient or deficient 1,25(OH)₂D, the active form of vitamin D, which indicates that 1,25(OH)₂D insufficiency or deficiency accelerates aging [13] and age-related diseases [14,15,20,22]. Our current findings suggest that intervertebral disc degeneration induced by 1,25(OH)₂D insufficiency is associated with aging accelerated by 1,25(OH)₂D insufficiency.

In this study, we found that expression levels of Prx1 and Sirt1 were not only down-regulated in NP tissues from 1,25(OH)₂D insufficient mice, but also up-regulated in NP tissues from Prx1-Sirt1 transgenic (Sirt1^{T8}) mice. These results provided sufficient rational for generating a mouse model that overexpressed Sirt1 in MSCs on a 1α(OH)ase^{+/-} background in order to investigate whether overexpression of Sirt1 in MSCs protects against IVDD induced by 1,25(OH)₂D insufficiency. By phenotypic analyses, we found that overexpression of Sirt1 in MSCs protected against 1,25(OH)₂D insufficiency-induced IVDD by up-regulating Sirt1 expression in NP tissues. A previous study has reported that the degenerative grade was negatively correlated with Sirt1 expression in IVDD [24]. The Sirt1 deficiency worsens IVDD, whereas the Sirt1 activator resveratrol protects against intervertebral disc injury by regulating cellular senescence and promoting regeneration [25]. Our recent study showed that 1,25(OH)₂D₃ up-regulated Sirt1 expression via VDR-mediated transcription, and overexpression of Sirt1 in MSCs protected against mandibular bone loss induced by 1,25(OH)₂D deficiency [29]. The results from our current study suggest that the 1,25(OH)₂D/Sirt1 axis may play an essential role in the pathogenesis of IVDD and might serve as a target in IVDD.

Sirt1 is an NAD⁺-dependent deacetylase with a wide range of substrates, such as p53, FOXO, NF-κB, and PGC-1α. Our previous studies demonstrated that Sirt1/FOXO3a axis plays an important role in the prevention of osteoporosis induced by Bmi1 or 1,25(OH)₂D deficiency in long bone or mandibles [26,27,29]. Another study has suggested that the Sirt1/p53 axis may play an essential role in diabetic intervertebral disc degeneration pathogenesis and therapeutics [32]. It has been reported that vitamin D retards IVDD through inactivation of the NF-κB pathway in mice [33]. However, it is unclear whether the NF-κB pathway inactivated by vitamin D is mediated via Sirt1. Under physiological and pathological conditions, NF-κB must undergo a variety of post-translational modifications, including phosphorylation and acetylation [34]. Acetylation (along with phosphorylation) plays a prominent role in regulating the nuclear action of NF-κB [35]. In this study, we found that 1,25(OH)₂D deficiency-induced IVDD by increasing acetylation and phosphorylation of p65 and activating the NF-κB inflammatory pathway, while overexpression of Sirt1 in MSCs prevented 1,25(OH)₂D deficiency-induced IVDD by decreasing acetylation and phosphorylation of p65 and inhibiting the NF-κB inflammatory pathway. To further determine whether the VDR or resveratrol activates Sirt1 to deacetylate p65 and inhibit its activity in NP cells, the VDR was knocked down in NP

cells and they were treated with or without resveratrol; the interactions between Sirt1 and acetylated p65 level and p65 nuclear localization were then examined using co-immunoprecipitation, Western blot, and immunofluorescence staining. Our results demonstrated that VDR knockdown reduced Sirt1 expression level, especially in the nucleus, significantly increased acetylated p65 levels and nuclear translocation in NP cells; in contrast, these effects were corrected in resveratrol treated VDR knockdown NP cells, suggesting that the VDR or resveratrol can activate Sirt1, reduce acetylated p65 levels and inactivate the NF-κB inflammatory pathway.

Current understanding of the mechanism of action of vitamin D involve binding of the active form, 1,25(OH)₂D, to the VDR, which for its genomic actions then binds to discrete regions of its target genes called vitamin D response elements. However, chromatin immunoprecipitation-sequencing studies have observed that the VDR can bind to many sites in the genome without its ligand [36]. VDR has a positive effect on inhibiting NF-κB-mediated inflammation, however, the underlying molecular mechanisms remain unclear. This study investigated whether 1,25(OH)₂D₃/VDR mediated via Sirt1 protects against NP cell degeneration by inhibiting the NF-κB inflammatory pathway. Thus, VDR-deficient NP cells were treated with 1,25(OH)₂D₃, or resveratrol or 1,25(OH)₂D₃ plus Ex527 (an inhibitor of Sirt1), and the alterations of cell proliferation and extracellular matrix proteins, Sirt1, TNF-α and IL-1β mRNA and protein expression, and the acetylation and phosphorylation levels of p65 were examined in NP cells using EdU assay, real-time RT-PCR, immunofluorescence staining and Western blots. Our results demonstrated that knockdown of VDR significantly reduced the proliferation and extracellular matrix protein synthesis of NP cells, significantly increased the senescence of NP cells with significantly downregulation of Sirt1 expression, upregulation of MMP13, TNF-α and IL-1β expression and increased the ratios of acetylated and phosphorylated p65/p65 in NP cells. The treatment of 1,25(OH)₂D₃ or resveratrol after VDR silencing partially rescued degeneration phenotypes of NP cells by up-regulating Sirt1 expression and inhibiting the NF-κB inflammatory pathway; these effects in NP cells were blocked by the inhibitor of Sirt1. Previous study has shown that the knockdown of VDR by using siRNA and dsRNA of VDR in vitro and in vivo led to more intense response of NF-κB signaling to lipopolysaccharide and higher level of apoptosis and autophagy, whereas 1,25(OH)₂D₃ stimulation after VDR silencing could partially alleviate apoptosis and induce autophagy [37]. Studies have revealed that IL-1β and TNF-α are inflammatory mediators that play a major role in the process of intervertebral disc degeneration, which can accelerate the apoptosis of intervertebral disc cells and induce the increase of MMPs in the NP [38]. The nature of the relationship between Sirt1 and NF-κB is antagonistic and, importantly, a direct association between Sirt1 and NF-κB has been established, in which Sirt1 is able to deacetylate the p65 subunit of NF-κB, triggering the transport of NF-κB from nucleus to cytoplasm and, therefore, suppressing its transcriptional activity [39]. Interestingly, some authors have established a possible association between the antagonistic relationship of Sirt1 and NF-κB in the hypothalamus, a central regulator in maintaining the metabolic energy balance in the body, and the generation of metabolic dysregulations in peripheral body tissues as potential sources of metabolic diseases [40]. Results from our study indicate that 1,25(OH)₂D/VDR mediated via Sirt1 protects against NP cell degeneration by inhibiting the NF-κB inflammatory pathway.

The role of regulated cell death (RCD) in IVDD has recently been

highlighted [41] as has the importance of N6-methyladenosine (m6A) modification in IVDD [42]. The role of the 1,25(OH)₂D/VDR system in regulating these mechanisms needs therefore to be identified as well as its action in concert with other modulators.

In summary, the results of this study for the first time demonstrated that 1,25(OH)₂D insufficiency accelerated intervertebral disc degeneration by reducing extracellular matrix protein synthesis and enhancing extracellular matrix protein degradation with reduced Sirt1 expression in NP tissues, whereas overexpression of Sirt1 in MSCs protected against 1,25(OH)₂D deficiency-induced intervertebral disc degeneration by decreasing acetylation and phosphorylation of p65 and inhibiting the NF-κB inflammatory pathway. In mechanistic studies, we demonstrated that knockdown of VDR significantly reduced the proliferation and extracellular matrix protein synthesis of NP cells, significantly increased the senescence of NP cells with significant downregulation of Sirt1 expression, upregulation of MMP13, TNF-α and IL-1β expression and increase in the ratios of acetylated and phosphorylated p65/p65 in NP cells. The treatment of 1,25(OH)₂D₃ or resveratrol after VDR silencing partially rescued degeneration phenotypes of NP cells by up-regulating Sirt1 expression and inhibiting NF-κB inflammatory pathway; these effects in NP cells were blocked by inhibitor of Sirt1. Results from this study indicate that 1,25(OH)₂D/VDR, mediated via Sirt1 protects against NP cell degeneration by inhibiting the NF-κB inflammatory pathway. This study provides new insights into the use of 1,25(OH)₂D₃ and Sirt1 agonists to prevent and treat intervertebral disc degeneration caused by vitamin D deficiency.

Funding

This work was supported by grants from the National Key R&D Program of China (2018YFA0800800), the National Natural Science Foundation of China (81730066) and the Canadian Institutes of Health Research (PJT-152963).

Declaration of competing interest

The authors declare that they have no known competing financial interests or personal relationships that could have appeared to influence the work reported in this paper.

References

- Oichi T, Taniguchi Y, Oshima Y, Tanaka S, Saito T. Pathomechanism of intervertebral disc degeneration. *JOR Spine* 2020;3(1):e1076.
- Tiosano D, Gepstein V. Vitamin D action: lessons learned from hereditary 1,25-dihydroxyvitamin-D-resistant rickets patients. *Curr Opin Endocrinol Diabetes Obes* 2012;19(6):452–9.
- Grubler MR, Gangler S, Egli A, Bischoff-Ferrari HA. Effects of vitamin D3 on glucose metabolism in patients with severe osteoarthritis: a randomized double-blind trial comparing daily 2000 with 800 IU vitamin D3. *Diabetes Obes Metabol* 2021;23(4):1011–9.
- Liao JL, Qin Q, Zhou YS, Ma RP, Zhou HC, Gu MR, et al. Vitamin D receptor Bsm I polymorphism and osteoporosis risk in postmenopausal women: a meta-analysis from 42 studies. *Genes Nutr* 2020;15(1):20.
- Steinfath M, Vogl S, Violet N, Schwarz F, Mielke H, Selhorst T, et al. Simple changes of individual studies can improve the reproducibility of the biomedical scientific process as a whole. *PLoS One* 2018;13(9):e0202762.
- Xu HW, Yi YY, Zhang SB, Hu T, Wang SJ, Zhao WD, et al. Does vitamin D status influence lumbar disc degeneration and low back pain in postmenopausal women? A retrospective single-center study. *Menopause* 2020;27(5):586–92.
- Biczo A, Szita J, McCall I, Varga PP, Genodisc C, Lazary A. Association of vitamin D receptor gene polymorphisms with disc degeneration. *Eur Spine J* 2020;29(3):596–604.
- Pekala PA, Jasinska M, Tattera D, Skoczen KM, Jarosz A, Konopka T, et al. Vitamin D receptor gene polymorphism influence on lumbar intervertebral disc degeneration. *Clin Anat* 2022;35(6):738–44.
- Mayer JE, Iatridis JC, Chan D, Qureshi SA, Gottesman O, Hecht AC. Genetic polymorphisms associated with intervertebral disc degeneration. *Spine J* 2013;13(3):299–317.
- Colombini A, Lanteri P, Lombardi G, Grasso D, Recordati C, Lovi A, et al. Metabolic effects of vitamin D active metabolites in monolayer and micromass cultures of nucleus pulposus and annulus fibrosus cells isolated from human intervertebral disc. *Int J Biochem Cell Biol* 2012;44(6):1019–30.
- Gruber HE, Hoelscher G, Ingram JA, Chow Y, Loeffler B, Hanley Jr EN. 1,25(OH)₂-vitamin D3 inhibits proliferation and decreases production of monocyte chemoattractant protein-1, thrombopoietin, VEGF, and angiogenin by human annulus cells in vitro. *Spine* 2008;33(7):755–65.
- Panda DK, Miao D, Tremblay ML, Sirois J, Farookhi R, Hendy GN, et al. Targeted ablation of the 25-hydroxyvitamin D 1alpha-hydroxylase enzyme: evidence for skeletal, reproductive, and immune dysfunction. *Proc Natl Acad Sci U S A* 2001;98(13):7498–503 [eng].
- Chen L, Yang R, Qiao W, Zhang W, Chen J, Mao L, et al. 1,25-Dihydroxyvitamin D exerts an antiaging role by activation of Nrf2-antioxidant signaling and inactivation of p16/p53-senescence signaling. *Aging Cell* 2019;18(3):e12951.
- Chen L, Yang R, Qiao W, Yuan X, Wang S, Goltzman D, et al. 1,25-Dihydroxy vitamin D prevents tumorigenesis by inhibiting oxidative stress and inducing tumor cellular senescence in mice. *Int J Cancer* 2018;143(2):368–82.
- Qiao W, Yu S, Sun H, Chen L, Wang R, Wu X, et al. 1,25-Dihydroxyvitamin D insufficiency accelerates age-related bone loss by increasing oxidative stress and cell senescence. *Am J Transl Res* 2020;12(2):507–18.
- Sun H, Qiao W, Cui M, Yang C, Wang R, Goltzman D, et al. The polycomb protein Bmi1 plays a crucial role in the prevention of 1,25(OH)₂D deficiency-induced bone loss. *J Bone Miner Res* 2020;35(3):583–95.
- Xue Y, Karaplis AC, Hendy GN, Goltzman D, Miao D. Genetic models show that parathyroid hormone and 1,25-dihydroxyvitamin D3 play distinct and synergistic roles in postnatal mineral ion homeostasis and skeletal development. *Hum Mol Genet* 2005;14(11):1515–28 [eng].
- Xue Y, Karaplis AC, Hendy GN, Goltzman D, Miao D. Exogenous 1,25-dihydroxyvitamin D3 exerts a skeletal anabolic effect and improves mineral ion homeostasis in mice that are homozygous for both the 1alpha-hydroxylase and parathyroid hormone null alleles. *Endocrinology* 2006;147(10):4801–10 [eng].
- Xue Y, Zhang Z, Karaplis AC, Hendy GN, Goltzman D, Miao D. Exogenous PTH-related protein and PTH improve mineral and skeletal status in 25-hydroxyvitamin D-1alpha-hydroxylase and PTH double knockout mice. *J Bone Miner Res* 2005;20(10):1766–77 [eng].
- Yang R, Chen J, Zhang J, Qin R, Wang R, Qiu Y, et al. 1,25-Dihydroxyvitamin D protects against age-related osteoporosis by a novel VDR-Ezh2-p16 signal axis. *Aging Cell* 2020;19(2):e13095.
- Yang R, Zhang J, Li J, Qin R, Chen J, Wang R, et al. Inhibition of Nrf2 degradation alleviates age-related osteoporosis induced by 1,25-Dihydroxyvitamin D deficiency. *Free Radic Biol Med* 2022;178:246–61.
- Yu S, Ren B, Chen H, Goltzman D, Yan J, Miao D. 1,25-Dihydroxyvitamin D deficiency induces sarcopenia by inducing skeletal muscle cell senescence. *Am J Transl Res* 2021;13(11):12638–49.
- Satoh A, Brace CS, Rensing N, Clifton P, Wozniak DF, Herzog ED, et al. Sirt1 extends life span and delays aging in mice through the regulation of Nk2 homeobox 1 in the DMH and LH. *Cell Metabol* 2013;18(3):416–30.
- Guo J, Shao M, Lu F, Jiang J, Xia X. Role of Sirt1 plays in nucleus pulposus cells and intervertebral disc degeneration. *Spine* 2017;42(13):E757–66.
- Xia X, Guo J, Lu F, Jiang J. SIRT1 plays a protective role in intervertebral disc degeneration in a puncture-induced rodent model. *Spine* 2015;40(9):E515–24.
- Sun W, Qiao W, Zhou B, Hu Z, Yan Q, Wu J, et al. Overexpression of Sirt1 in mesenchymal stem cells protects against bone loss in mice by FOXO3a deacetylation and oxidative stress inhibition. *Metabolism* 2018;88:61–71.
- Wang H, Hu Z, Wu J, Mei Y, Zhang Q, Zhang H, et al. Sirt1 promotes osteogenic differentiation and increases alveolar bone mass via Bmi1 activation in mice. *J Bone Miner Res* 2019;34(6):1169–81.
- Arkesteijn IT, Smolders LA, Spillekom S, Riemers FM, Potier E, Meij BP, et al. Effect of coculturing canine notochordal, nucleus pulposus and mesenchymal stromal cells for intervertebral disc regeneration. *Arthritis Res Ther* 2015;17:60.
- Chen H, Hu X, Yang R, Wu G, Tan Q, Goltzman D, et al. SIRT1/FOXO3a axis plays an important role in the prevention of mandibular bone loss induced by 1,25(OH)₂D deficiency. *Int J Biol Sci* 2020;16(14):2712–26.
- Chen JW, Ni BB, Li B, Yang YH, Jiang SD, Jiang LS. The responses of autophagy and apoptosis to oxidative stress in nucleus pulposus cells: implications for disc degeneration. *Cell Physiol Biochem* 2014;34(4):1175–89.
- Cheng Z, Xiang Q, Wang J, Zhang Y. The potential role of melatonin in retarding intervertebral disc ageing and degeneration: a systematic review. *Ageing Res Rev* 2021;70:101394.
- Zhang Z, Lin J, Nisar M, Chen T, Xu T, Zheng G, et al. The Sirt1/P53 Axis in diabetic intervertebral disc degeneration pathogenesis and therapeutics. *Oxid Med Cell Longev* 2019;2019:7959573.
- Huang H, Cheng S, Zheng T, Ye Y, Ye A, Zhu S, et al. Vitamin D retards intervertebral disc degeneration through inactivation of the NF-kappaB pathway in mice. *Am J Transl Res* 2019;11(4):2496–506.
- Chen LF, Williams SA, Mu Y, Nakano H, Duerr JM, Buckbinder L, et al. NF-kappaB RelA phosphorylation regulates RelA acetylation. *Mol Cell Biol* 2005;25(18):7966–75.
- Chen LF, Mu Y, Greene WC. Acetylation of RelA at discrete sites regulates distinct nuclear functions of NF-kappaB. *EMBO J* 2002;21(23):6539–48.
- Bikle DD. Ligand-independent actions of the vitamin D receptor: more questions than answers. *JBMR Plus* 2021;5(12):e10578.
- Huang D, Guo Y, Li X, Pan M, Liu J, Zhang W, et al. Vitamin D3/VDR inhibits inflammation through NF-kappaB pathway accompanied by resisting apoptosis and inducing autophagy in abalone *Haliotis discus hannai*. *Cell Biol Toxicol* 2021.
- Podichetty VK. The aging spine: the role of inflammatory mediators in intervertebral disc degeneration. *Cell Mol Biol (Noisy-le-grand)* 2007;53(5):4–18.

- [39] de Gregorio E, Colell A, Morales A, Mari M. Relevance of SIRT1-NF-kappaB Axis as therapeutic target to ameliorate inflammation in liver disease. *Int J Mol Sci* 2020; 21(11).
- [40] Kauppinen A, Suuronen T, Ojala J, Kaarniranta K, Salminen A. Antagonistic crosstalk between NF-kappaB and SIRT1 in the regulation of inflammation and metabolic disorders. *Cell Signal* 2013;25(10):1939–48.
- [41] Yang F, Liu W, Huang Y, Yang S, Shao Z, Cai X, et al. Regulated cell death: implications for intervertebral disc degeneration and therapy. *J Orthop Translat* 2022;37:163–72.
- [42] Zhu B, Chen HX, Li S, Tan JH, Xie Y, Zou MX, et al. Comprehensive analysis of N6-methyladenosine (m(6)A) modification during the degeneration of lumbar intervertebral disc in mice. *J Orthop Translat* 2021;31:126–38.